PROCEEDINGS OF SPIE

SPIEDigitalLibrary.org/conference-proceedings-of-spie

End-to-end tests of the TuMag instrument for the SUNRISE III mission

Alberto Álvarez Herrero, Daniel Garranzo-García, Armonía Núnez, Manuel Silva-López, Antonio Campos-Jara, et al.

Alberto Álvarez Herrero, Daniel Garranzo-García, Armonía Núnez, Manuel Silva-López, Antonio Campos-Jara, Pilar García Parejo, María Cebollero, Julia Atienzar, Francisco J. Bailén, Julian Blanco Rodríguez, Pablo Santamarina, David Orozco Suárez, Jose Carlos del Toro Iniesta, "End-to-end tests of the TuMag instrument for the SUNRISE III mission," Proc. SPIE 12184, Ground-based and Airborne Instrumentation for Astronomy IX, 121842F (29 August 2022); doi: 10.1117/12.2629272

SPIE.

Event: SPIE Astronomical Telescopes + Instrumentation, 2022, Montréal, Québec, Canada

End-to-end tests of the TuMag instrument for the SUNRISE III mission

Alberto Alvarez-Herrero*[a], Daniel Garranzo-García[a], Armonía Núñez[a], Manuel Silva-López[a], Antonio Campos-Jara[a], Pilar García Parejo[a], María Cebollero[b], Julia Atienzar[c], Francisco J. Bailén[c], Julián Blanco Rodríguez[d], Pablo Santamarina[c], David Orozco Suárez[c], Jose Carlos del Toro Iniesta[c]
[a]Instituto Nacional de Técnica Aeroespacial (INTA), Carretera de Ajalvir Km4, 28850 Madrid, Spain; [b]Ingeniería de Sistemas para la Defensa de España (ISDEFE), C. de Beatriz de Bobadilla 3, 28040 Madrid; [c]Instituto de Astrofísica de Andalucía (IAA-CSIC), Apartado de Correos 3004, 18080 Granada, Spain; [d]Universitat de València, Catedrático José Beltrán 2, 46980 Paterna-Valencia, Spain.

ABSTRACT

SUNRISE III mission is a one-meter aperture telescope onboard a balloon within NASA Long Duration Balloon Program. Three post-focus instruments are used for studying the Sun's dynamics and magnetism, among which the Tunable Magnetograph (TuMag) is a tunable imaging spectropolarimeter.

TuMag is a diffraction-limited imager, a high sensitivity polarimeter ($< 10^{-3}$), and a high-resolution spectrometer ($\Delta\lambda \sim 65$ mÅ). It will be able to study solar magnetic fields at high spatial resolution (~100 km on the solar surface). It will make images of the solar surface magnetic field after measuring the state of polarization of light within three selected spectral lines: the Fe I lines at 525.02 nm and 525.06 nm, and the Mg I b2 line at 517.27 nm. It will be sensitive to the solar vector magnetic fields and line-of-sight velocities, in the photospheric and chromospheric layers. TuMag will be the first solar magnetograph onboard an aerospace platform with the capability of tuning the solar line to be observed.

In this paper the TuMag end-to-end tests carried out during the verification phase are described. These tests are performed to characterize and calibrate the instrument. Specifically, they determine the polarimetric and spectroscopic performances of the instrument as well as the image quality. The availability of a singular facility, an ISO6 clean room with a coelostat on the building roof, allowed the use of solar light during the verification campaign. This was key to a complete instrument verification due to the unique spectroscopic and polarimetric characteristics of solar light.

Keywords: Solar physics, instrumentation, imager, polarimeter, spectrometer, coelostat, liquid crystals, etalon.

1. INTRODUCTION

SUNRISE III is a balloon-borne solar observatory dedicated to the investigation of the key processes governing the physics of the magnetic field and the convective plasma flows in the lower solar atmosphere. SUNRISE III flew within the NASA Long Duration Balloon Program on July 10, 2022, even though it could not finish its flight unfortunately. Specifically, it consists of one-meter aperture telescope with three post-focus instruments. One of them is TuMag (Tunable Magnetograph): a tunable imaging spectropolarimeter in the visible wavelengths. It provides polarized images of a 60″× 60″ field of view (FoV) of the Sun in four polarization states. These images can later be processed on ground to retrieve maps of the solar physical quantities of interest.

Specifically, TuMag is a diffraction-limited imager, a high sensitivity polarimeter ($<10^{-3}$) and a high resolution spectrometer ($\Delta\sim$ 65 mÅ). It will make images of the solar surface magnetic field and line-of-sight velocity of the photosphere and the lower chromosphere after measuring the state of polarization of light within three selected spectral lines: the Fe I lines at 525.02 nm and 525.06 nm, and the Mg I b2 line at 517.27 nm. It should be highlighted that TuMag is the first solar magnetograph onboard an aerospace platform with the capability of tuning the solar line to be observed. Further technical details about TuMag can be found in [1].

*alvareza@inta.es; phone +34 91 520 1062; www.inta.es

Ground-based and Airborne Instrumentation for Astronomy IX, edited by Christopher J. Evans, Julia J. Bryant, Kentaro Motohara, Proc. of SPIE Vol. 12184, 121842F
 · 0277-786X · doi: 10.1117/12.2629272

TuMag is a fully new instrument based on the heritage of the development carried out for the successful IMaX (The Imaging Magnetograph eXperiment) for the SUNRISE I and II missions [2–4]. Also, TuMag is profited of the background obtained during the development of the Polarimetric and Helioseismic Imager (PHI) for the ESA and NASA Solar Orbiter mission[5].

In this paper, the methods carried out and the corresponding results obtained to verify that the instrument fulfils the requirements after being integrated and assembled are described. In particular, the end-to-end (E2E) tests to check the imaging quality as well as the polarimetric and spectroscopic performances are explained. The E2E tests are carried out with the full system working as similar as possible to the operational case, i.e.: Optical Unit, Electronic Unit, external harness and software in flight configuration.

The auxiliary optical instrumentation used, specially designed in most of the cases, is described in Section 2. This is the so-called Optical Ground Support Equipment (OGSE). The use of a singular facility should be pointed out: an ISO-6 clean room with a coelostat installed in its roof to have a controlled sun light beam in a controlled particulate and molecular contamination environment. In Section 3 the results obtained for the E2E tests are described and discussed.

2. EXPERIMENTAL DETAILS

2.1 OGSE for the image E2E test

A specific image E2E test was carried out to verify the TuMag image quality as the final stage of the Assembly, Integration and Verification (AIV) phase. In order to check TuMag electro-optical performances (resolution, magnification, distortion, etc.) a specific OGSE was required to simulate the optical system that feeds TuMag in SUNRISE III: the telescope and the ISLiD (Image Stabilization and Light Distribution) system.

The OGSE was an optical relay in finite-conjugate configuration to project four different targets at TuMag entrance field stop (F4 frame). F4 is an intermediate telescope-ISLiD focus and the established optical interface for TuMag.

Figure 1 shows the different elements that compose it (from Thorlabs Inc.):

- 525 nm diode, as illumination source (SOLIS-525C model).
- Diffuser (ED1-C20-MD model).
- Targets: USAF, star, slit and grid.
- Achromatic doublet of 500 mm focal length (AC254-500-A model).
- Variable diaphragm (CP20S model).
- Achromatic doublet of 300 mm focal length (AC254-300-A model).

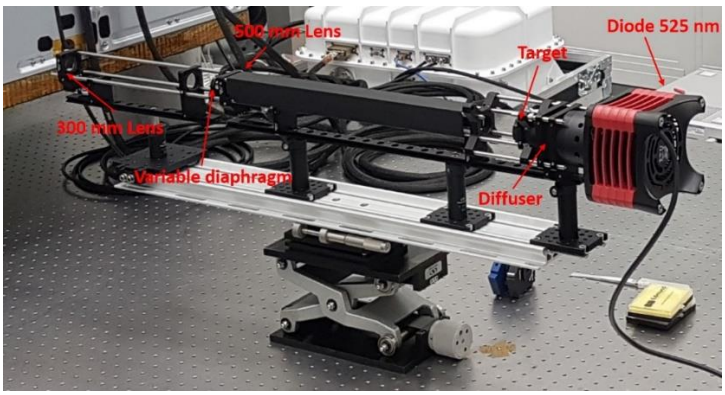

Figure 1. OGSE for the Image E2E test.

The focal lengths of the lenses were chosen to have a target´s magnification <1 (specifically 0.6) at TuMag's F4. Thus, a sub-pixel slit image (TuMag pixel size = 11 μm) could be taken at the TuMag' focal plane (taking into account the nominal TuMag magnification of 2.47).

Additionally, the projection part of the OGSE had a diaphragm of 12.4 mm diameter positioned at the focus point of the 300 mm achromatic lens. In this way two things were achieved: having an F# of 24.2 at the TuMag' entrance and obtaining telecentric light cones at TuMag' F4 Frame (as SUNRISE III telescope and ISLiD system work).

A theodolite was used to aid in the position of the targets at the focus point of the 500 mm lens.

Each target was chosen to aid in the verification of the main TuMag electro-optical performances at the best focus position. For example, with the USAF and Star test targets, the TuMag image contrast was analyzed for several target frequencies (image resolution) as well as the magnification. The slit target allowed to calculate the Modulation Transfer Function (MTF), the Strehl ratio and the wavefront error. In addition, the grid target shown an estimation of the distortion and the image scale.

In Section 3.1, only the results obtained from the USAF and slit targets will be presented. The USAF target was the 1951 USAF negative resolution test target from Thorlabs Inc. (R1DS1N model). The target has 6 groups (+2 to +7) with 6 elements, offering a maximum resolution of 228.0 line pairs (one light line and one dark line) per millimeter. Because this target features sets of three lines, it reduces the occurrence of spurious resolution and thus help prevent inaccurate resolution measurements. The slit target was the mounted optical slit S5K model (from Thorlabs Inc.) with 5±1 μm wide and 3 mm long.

Note that the slit target allows an accurate determination of the system MTF using the slanted-slit method described elsewhere[6–8]. On the other hand, the USAF target allows a fast diagnostic of the instrument health (i.e.: after TuMag environmental tests, transport, etc.) looking for the higher resolution group that the instrument can resolve.

In addition to these methods, the TuMag image optical quality was determined using the phase diversity technique[9]. TuMag includes a calibrated defocusing plate that can be inserted in the optical path in order to deduce the Point Spread Function (PSF) during the flight and it allows to carry out image restauration by deconvolution[1]. The results obtained from the phase diversity technique are in agreement with the results shown in Section 3.1, but they are out of the scope of this work.

2.2 OGSE for the polarimetric E2E test

The OGSE for the polarimetric test was carried out also using an optical relay in finite-conjugate configuration (Figure 2) with a Polarization Stage Generator (PSG). Two achromatic doublets of 200 mm and 300 mm focal length (AC508-200-A model and AC254-300-A model from Thorlabs Inc., respectively) were selected for this optical system. The same laser diode centered at 525 nm described in the previous Section was used as light source.

Two types of PSG were used. The first PSG consisted of a linear polarizer (LP) and a rotating quarter-waveplate (QWP), introducing a total of 73 known polarization states of the light to calibrate the Polarization Modulation Package. The polarizer and the QWP were located between the object and the lens and the incidence angles on them were under their acceptance angles in order to guarantee a homogeneous polarization state over the full FoV.

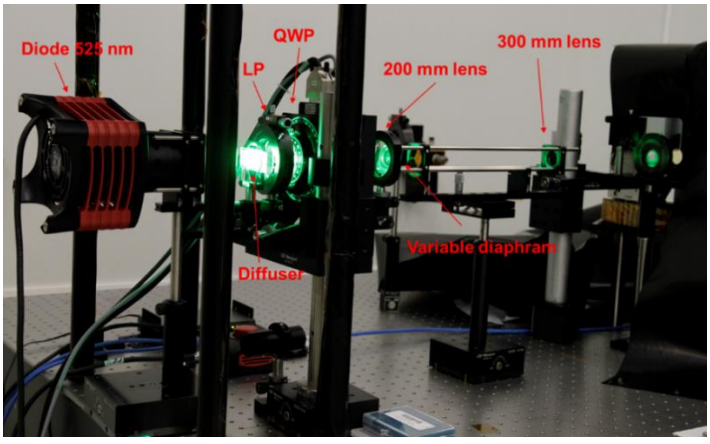

Figure 2. OGSE for the polarimetric E2E test with the Polarization Stage Generator (PSG) consisting of a linear polarizer (LP) and a rotating quarter-waveplate (QWP).

The LP was a high performance glass linear polarizer from Edmund Optics. The retardance of the QWP (10RP34-6328 from Newport, zero-order polymer wave-plate), originally designed for λ = 632.8 nm, was measured at that interest wavelength with a Variable Angle Spectroscopic Ellipsometry (VASE) from J.A Woollam, obtaining a value of 0.2588 λ within an acceptance angle of ±10 deg. That means a retarder value of 0.3081 λ for λ = 525 nm, the wavelength of interest. Note that this value in the optimum range (0.3073 λ-0.3661 λ) for minimization of the rms error and the maximization of the SNR (Signal to Noise Ratio) of the calibration measurement[10]. An object diffuser was used in order to homogenize the illumination.

The second PSG consisted of an eigenstate calibration set for λ = 525 nm from Meadowlark Optics located before the TuMag optical entrance and after the OGSE for the image E2E test explained in Section 2.1. This system was used as a reduced polarimetric test for an easily portable setup and a fast check of the TuMag polarimetric performances during the different stages of the solar observatory assembly. This second PSG has a vignetting effect and just the central area of the TuMag FoV can be checked, but it is enough for a fast diagnostic test.

2.3 OGSE for the spectroscopic E2E test

In order to perform an accurate spectroscopic verification we have used direct sunlight as input for TuMag. The clean room has available windows that, after a few mirror reflections, allow Sun illumination by means of a coelostat. This enables the verification of the actual solar absorption lines of interest, i.e. the TuMag science wavelengths. A set of folding mirrors and an imaging system were place in the incoming solar beam from the coelostat. The imaging system of this OGSE has a diaphragm with a diameter of 42 mm placed at the focus point of an achromatic doublet with a 1000 mm focal length (AC508-1000-A-ML from Thorlabs Inc.). As a consequence, the illumination system is telecentric at F4 with an F# < 24.2 and it mimics the SUNRISE III telescope and ISLiD feed to TuMag as explained previously. The Sun image at F4 has a 9.6 mm diameter size. Figure 3 shows an image of the coelostat at the roof of the building that hosts the clean room as well as the optical system in the ISO 6 clean room.

Figure 3. Up) INTA coelostat. The stabilized Sun light is directed towards the clean room. Bottom) Folding mirrors and imaging system in ISO6 clean room.

Similarly to the other E2E tests, a portable setup for a fast instrument health diagnostic was designed. It consisted of the OGSE for the image E2E test and a calibrated iodine cell from Bureau International des Poids et Mesures (Figure 4). Since the absorption peaks of the iodine are well known and characterized[11], they are very useful for wavelength calibrations[2,12].

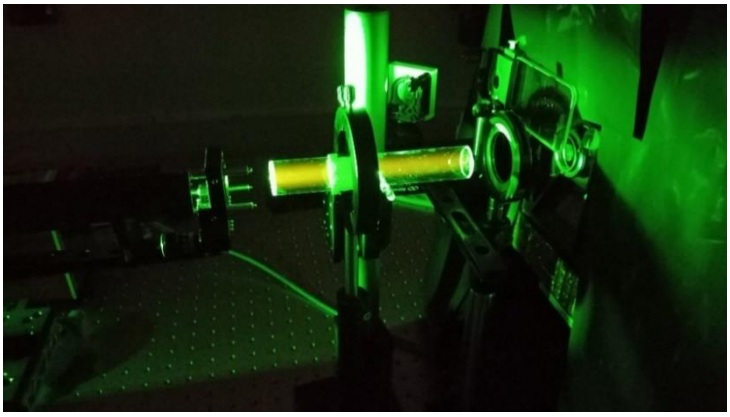

Figure 4. Detail of the OGSE showing the iodine cell illuminated by the green LED at TuMag entrance.

3. RESULTS AND DISCUSSION

3.1 Image E2E test results

The main Image E2E test results obtained with the USAF test and slit targets are presented below. The TuMag electro-optical performances were analyzed at the previously determined best focus position. Since TuMag cameras were in a fixed position, a throughfocus of the target projection by the OGSE on TuMag F4 was carried out. The best focus position was established as the location with the highest image contrast, *C*, defined as:

$$C = \frac{I_{std}}{I_{mean}}, \tag{1}$$

where I_{mean} is the average of the counts across the image and I_{std} is the standard deviation.

Magnification was defined as the ratio between the sizes of the image and the object (USAF test, in this case). Therefore, the magnification can be express according to the spatial frequencies as:

$$m_{TuMag} = \frac{\nu_{obj}}{m_{OGSE^*}\,\nu_{imag}} \tag{2}$$

Where ν_{obj} is the spatial frequency of the USAF' element under study, m_{OGSE} is the magnification of the OGSE (0.6) and ν_{imag} is the resulting spatial frequency in the image plane of TuMag.

The image spatial frequencies of all USAF Groups 2 elements (vertical and horizontal bars) were calculated and compared with their corresponding object spatial frequencies. Previously, the images were corrected with flat and dark images before analyzing. Table 1 shows the magnification obtained with each Narrow Bandpass Filter (NBF) and for both TuMag cameras.

Table 1.Magnifications obtained for each Narrow Band Pass Filter (NBF) and orientation.

Wavelength	Magnification	Camera 1	Camera 2
NBF3: 517.27 nm	Vertical	2.471	2.471
	Horizontal	2.472	2.474
NBF1: 525.02 nm	Vertical	2.469	2.469
	Horizontal	2.471	2.472
NBF2: 525.06 nm	Vertical	2.470	2.470
	Horizontal	2.472	2.472

The image resolution of TuMag was evaluated by means of the Contrast Transfer Function (CTF) obtained from the analysis of the USAF test groups. Anyway, the results are not presented here for the sake of brevity, because the MFT results obtained with the slant-slit method are considered more relevant and they are in agreement.

The most interesting element corresponds to the USAF test Group 5-Element 2, which corresponds to 35.9 lp/mm, and that it is translated to 24.3 lp/mm in the image. This is close to the Airy disk radius of 26.4 lp/mm, and therefore, the maximum TuMag image resolution. Figure 5 shows the images of the USAF test Group 5 obtained with the different NBFs. The Group 5-Element 2 is clearly resolved with the 517.27 nm NBF3 and the differences between vertical and horizontal CTF values are minimal. The resolution for 525.02 nm and 525.06 nm NBFs is lower than that of the 517.27 nm NBF and shows larger differences between vertical and horizontal CTF values.

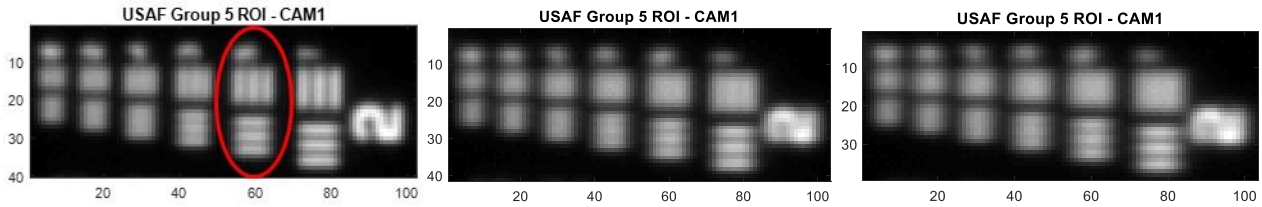

Figure 5. Images of the USAF test Group 5 with the NBFs: 517.27 nm (left), 525.02 nm (center) and 525.06 nm (right)

The TuMag image quality was evaluated for the slit target images through the Modulation Transfer Function (MTF) calculated as the real part of the Line Spread Function (LSF)' Fourier transform using the slant-slit method[8].

The results obtained from the image MTFs up to 32 lp/mm (cutoff frequency) are presented. Figure 6, Figure 7 and Figure 8 show the comparison between the experimental and the expected MTF curve from the design for the three NBFs and the two TuMag cameras.

From Figures 6-8, it can be seen that the image resolution for 517.27 nm NBF is achieved for both the horizontal and vertical slits. In the case of 525.02 nm and 525.06 nm NBFs, the resolution for the horizontal slit is achieved but for the vertical slit it is lower than expected. These results agree with those observed with the USAF test shown above.

In theory, some astigmatism was expected due to the etalon which wavefront error was previously and separately measured. Nevertheless, the results show a higher difference between the horizontal and vertical MTFs. In addition, it was observed that the higher the tuning Angle Of Incidence (AOI) of the NBF, the higher the MTF decay. One possible explanation is related to the method used to hold the NBFs in the Filter Wheel[13] used to insert them in the optical path which could have introduced certain deformations in them.

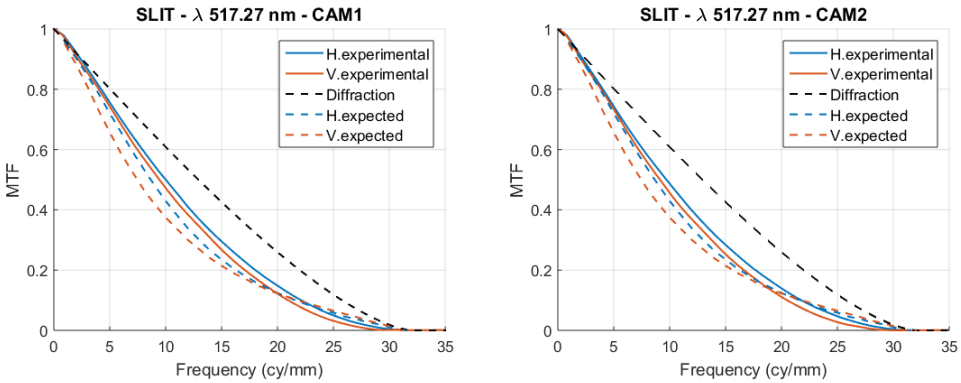

Figure 6. MTF values of the slit target image for 517.27 nm NBF3 taken with camera 1 (left) and camera 2 (right)

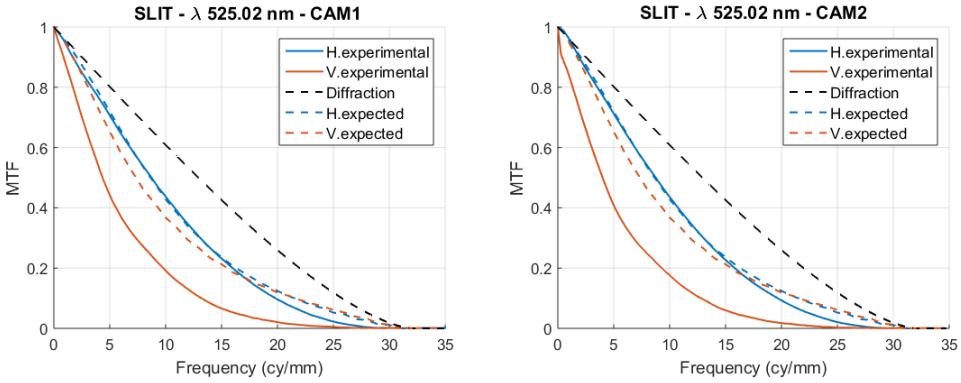

Figure 7. MTF values of the slit target image for 525.02 nm NBF1 taken with camera 1 (left) and camera 2 (right)

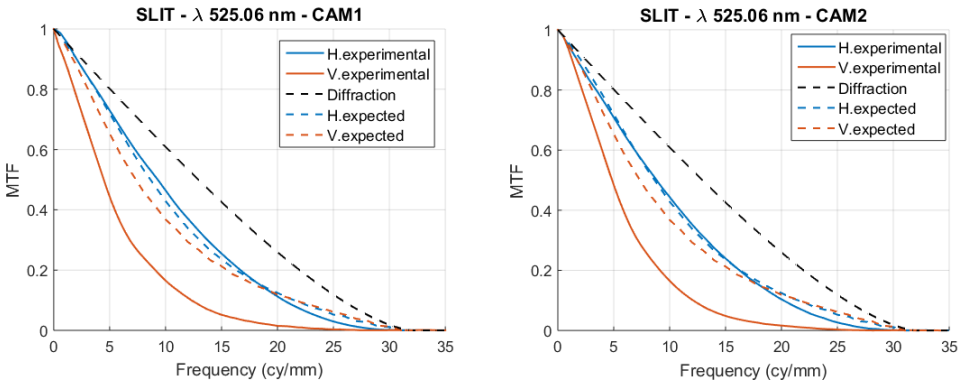

Figure 8. MTF values of the slit target image for 525.06 nm NBF2 taken with camera 1 (left) and camera 2 (right)

The image Strehl ratio, *R*, was calculated as the ratio between the actual MTF values obtained with the slit target images and the TuMag diffraction MTF, according to the following equation.

$$R = \frac{\int \mathrm{MTF}_{\mathrm{actual}}}{\int \mathrm{MTF}_{\mathrm{diffraction}}} \tag{3}$$

Table 2 shows the Strehl ratio values obtained of the horizontal and vertical slit images for the three NBFs and both TuMag cameras.

Table 2. Strehl ratio summary.

Wavelength	Strehl ratio	Camera 1	Camera 2
NBF3: 517.27 nm	Horizontal	0.826	0.806
	Vertical	0.782	0.761
NBF1: 525.02 nm	Horizontal	0.725	0.726
	Vertical	0.436	0.405
NBF2: 525.06 nm	Horizontal	0.764	0.736
	Vertical	0.451	0.444

Subsequently, an estimation of the wavefront error (WFE) was obtained considering its relationship with the Strehl ratio.

$$R = \mathrm{e}^{-(2\pi \mathrm{WFE})^2} \tag{4}$$

Table 3 shows the calculated WFE from the horizontal and vertical Strehl ratio values obtained with the slit target images for the three NBFs and both cameras.

Table 3. Wavefront error summary.

Wavelength	WFE	Camera 1	Camera 2
NBF3: 517.27 nm	Horizontal	0.069 (λ/14.5)	0.074 (λ/13.5)
	Vertical	0.079 (λ/12.7)	0.083 (λ/12.1)
NBF1: 525.02 nm	Horizontal	0.090 (λ/11.1)	0.090 (λ/11.1)
	Vertical	0.145 (λ/6.9)	0.151 (λ/6.6)
NBF2: 525.06 nm	Horizontal	0.082 (λ/12.1)	0.088 (λ/11.3)
	Vertical	0.142 (λ/7.0)	0.143 (λ/7.0)

These Strehl ratio and WFE values were compared to those expected in the worst case, 0.593 and 0.115 (λ/8.7) respectively. Again, the drop in resolution is observed in the image of the vertical slit target for the 525 nm NBFs.

As mentioned previously, the use of the phase diversity technique allowed to confirm these results as well as the image restauration achieving the required diffraction-limited quality.

3.2 Polarimetric E2E test results

The polarimetric calibration was carried out at 35ºC at the three wavelengths of the instrument (517.27, 525.02 and 525.06 nm) and the two cameras. An optimum modulation scheme that maximizes the polarimetric efficiencies was selected[1] and is shown in the following Table 4:

Table 4. LCVRs retardances of the polarization modulation scheme

Modulation	$LCVR_1$ [deg]	$LCVR_2$ [deg]
1	ρ_1 = 225	σ_1=234.74
2	ρ_1= 225	σ_2=125.26
3	ρ_2= 315	σ_3=54.74
4	ρ_2= 315	σ_4=305.26

The initial voltages applied to the LCVR cells corresponds to the retardances of the polarization modulation scheme obtained from the individual calibration of the LCVRs carried out in a Woollam Variable Angle Spectroscopic Ellipsometer (VASE) at the three instrument wavelengths. Nevertheless, deviations from an ideal system caused by manufacturing tolerances of the optical elements and the mechanical assembly, azimuthal angles among the polarizing elements (LCVRs, polarizer, etc) different from the designed, LCVR non-ideal effects and the instrumental residual polarization can cause polarization modulation different from the theoretical ideal system. A fine-tuning process[14] was carried out in order to optimize the polarimetric efficiencies of the system. The polarimetric efficiencies achieved with this method, shown in Figure 9, are very high, fulfilling by far the TuMag polarimetric modulation efficiencies, ε, requirement: [0.95 0.45 0.45 0.45]. Note that the theoretical maximum modulation efficiencies[15] are [1 0.577 0.577 0.577].

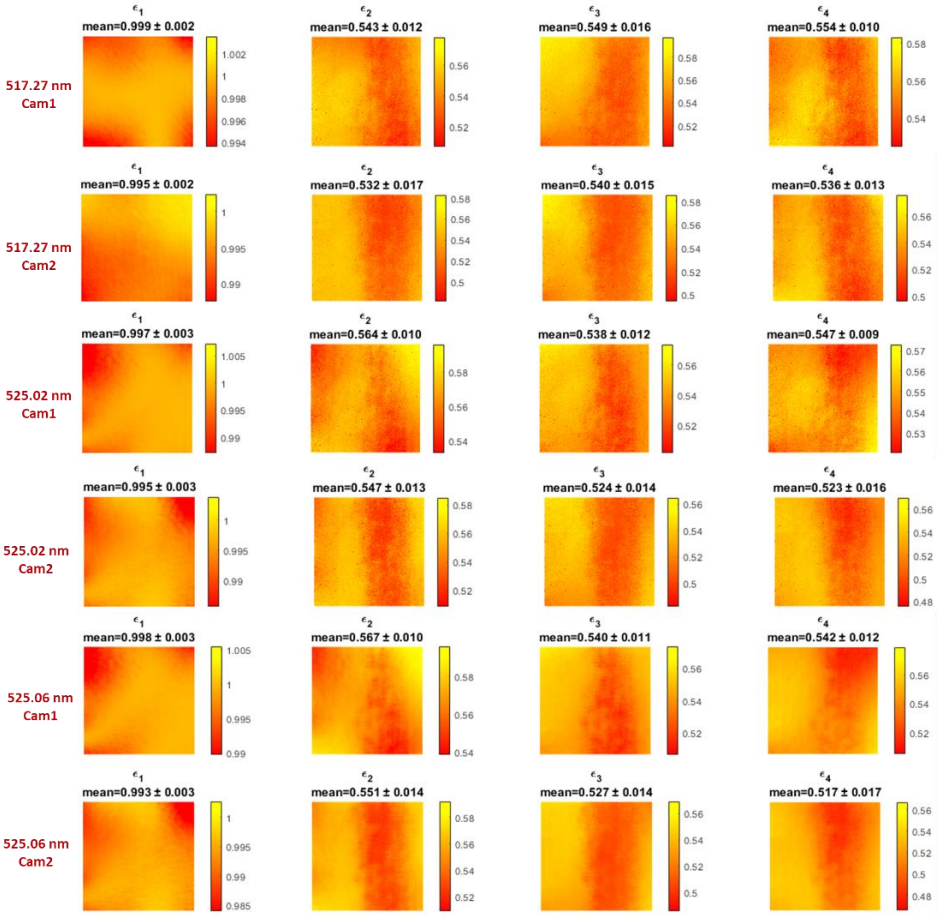

Figure 9. Polarimetric modulation efficiencies at T=35°C measured pixel-by-pixel for the full TuMag FoV. It was measured for the three NBFs and the two cameras.

The polarimetric modulation efficiencies shown in Figure 9 are higher than the 90% of the theoretical maximum and they are homogeneous across the FoV as the standard deviation values shows. Anyway, a pixel-by pixel polarimetric modulation matrix was obtained and it can be applied pixel-by-pixel to improve the TuMag polarimetric accuracy.

3.3 Spectroscopic E2E test results

Spectral measurements using Sun light at each target wavelength line are shown in Figure 10. These are spectral (voltage) scans performed with the etalon, using each NBF at the corresponding temperature set-point (27 ºC ± 0.5 ºC). The whole voltage range corresponds to ~1.13 Å. The absorption lines of interest are clearly seen in every measurement. The distortion is mostly related to the poor seeing conditions at the time of the test.

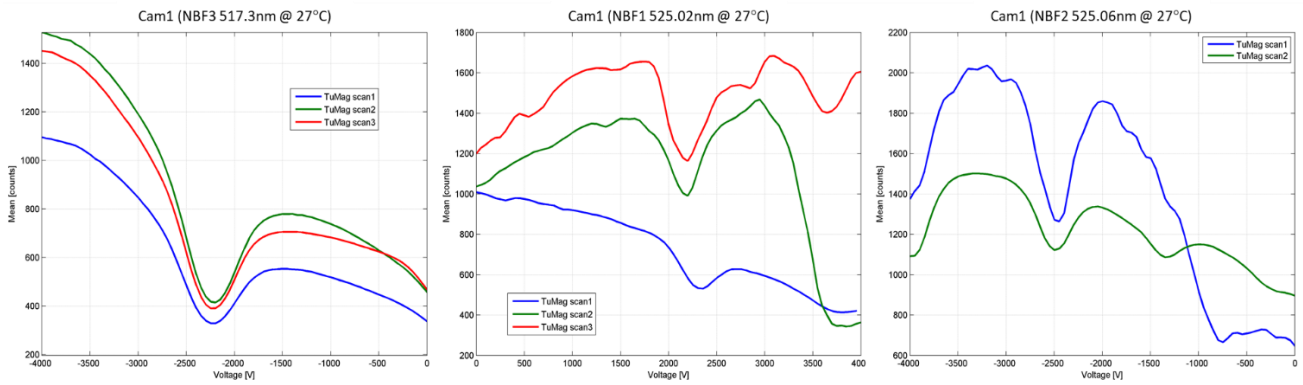

Figure 10. Spectral measurements performed using Sun light. The etalon is voltage scanned along each NBF transmission band. The solar absorption lines are clearly resolved.

A fast spectral verification can be seen in Figure 11. Here we have employed the OGSE with the iodine cell. The actual measurements are plotted against a simulated iodine spectrum. This simulated spectrum was generated by convolution of the iodine spectrum with the etalon transmission profile. This profile, an Airy function of double etalon pass, was modelled as a Lorentzian profile with FWHM peak of 8.7 pm (87 mÅ), as nominally specified. As illustrated, there is a good match in the spectral range of the NBFs transmission band. Overall these measurements verify that, for every NBF, the spectral bandpass is better than 10 pm FWHM and the spectral resolution is larger than 50000, as required.

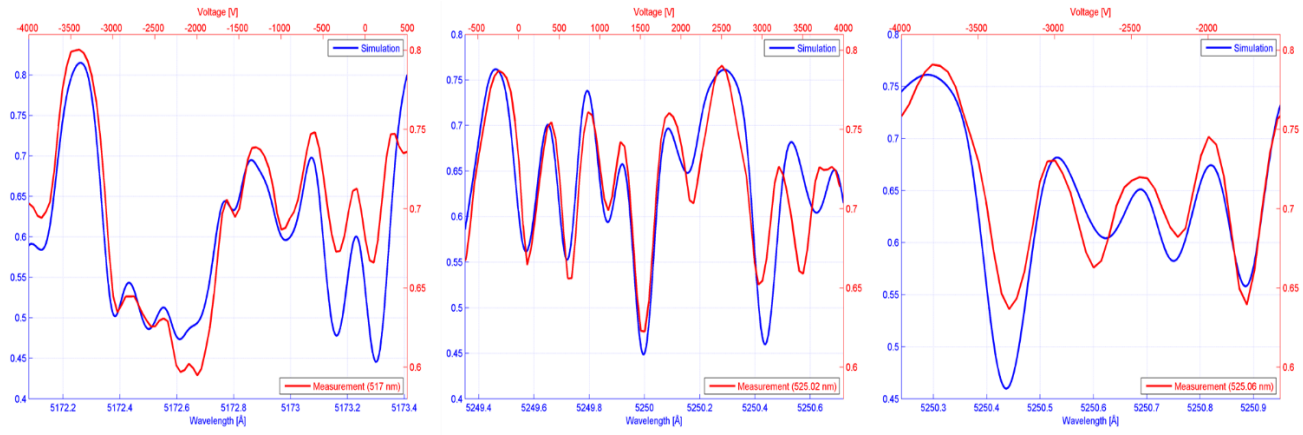

Figure 11. Spectral measurements performed using the OGSE with the iodine cell. The spectral signature, obtained after NBFs transmission correction, matches a simulation of the iodine spectrum convolved with the etalon.

Finally, and according to the plots shown, the V/Å constant found for each NBF is summarized in the next Table:

Table 5. Tuning constant for each NBF.

NBF	NBF3: 517.27 nm	NBF1: 525.02 nm	NBF2: 525.06 nm
Tuning constant	3401 V/Å	3211 V/Å	3515 V/Å

4. CONCLUSIONS

The end-to-end tests carried out to verify that the TuMag instrument fulfils the requirements after being integrated and assembled were described. Specifically, the TuMag image quality as well as the polarimetric and spectroscopic performances were determined. Additionally to the detailed version of the tests, a reduced test of each one was defined in order to allow a fast diagnostic of the instrument health with a portable setup during all the phases of the solar observatory assembly (i.e.: after TuMag environmental tests, transport, etc.). Besides, the optical setup used for each specific end-to-end test has been presented.

The results obtained show that TuMag fulfill the challenging requirements of this tunable imaging spectropolarimeter, the first one with the capability of tuning the solar line to be observed from an aerospace platform. The MTF values and the spatial resolution are in concordance with the design guaranteeing that the diffraction-limited optical quality can be achieved using the phase diversity technique. Polarimetric modulation efficiencies higher than 90% of the theoretical maximum were found across the instrument FoV. Finally, the TuMag spectral resolution is better than 10 pm FWHM and the spectral resolution is larger than 50000, as required.

ACKNOWLEDGMENTS

The authors would like to thank Ministerio de Ciencia e Innovación from the Spanish government for the support of this research via the grant Space Solar Physics RTI2018-096886-B-C5 and "Centro de Excelencia Severo Ochoa" grant SEV-2017-0709.

REFERENCES

[1] Álvarez-Herrero, A., Fernandez-Medina, A., Cebollero, M., Garranzo-García, D., Núñez, A., Gonzalo, A., Sánchez, A., Villanueva, J., Garcia-Parejo, P., Campos-Jara, A., Silva-Lopez, M., San Julián, R. and Laguna, H., "TuMag for SUNRISE III mission: development of the optical unit of an imaging spectropolarimeter," Proc. SPIE Astronomical Telescopes & Instrumentation, to be published (2022).

[2] Martínez Pillet, V., Iniesta, J. C. del T., Álvarez-Herrero, A., Domingo, V., Bonet, J. A., González Fernández, L., López Jiménez, A., Pastor, C., Gasent Blesa, J. L., Mellado, P., Piqueras, J., Aparicio, B., Balaguer, M., Ballesteros, E., Belenguer, T., Bellot Rubio, L. R., Berkefeld, T., Collados, M., Deutsch, W., et al., "The Imaging Magnetograph eXperiment (IMaX) for the Sunrise Balloon-Borne Solar Observatory," Sol Phys **268**(1), 57–102 (2010).

[3] Barthol, P., Gandorfer, A., Solanki, S. K., Schüssler, M., Chares, B., Curdt, W., Deutsch, W., Feller, A., Germerott, D., Grauf, B., and others., "The sunrise mission," Solar Physics **268**(1), 1–34 (2011).

[4] Solanki, S. K., Riethmüller, T. L., Barthol, P., Danilovic, S., Deutsch, W., Doerr, H.-P., Feller, A., Gandorfer, A., Germerott, D., Gizon, L., Grauf, B., Heerlein, K., Hirzberger, J., Kolleck, M., Lagg, A., Meller, R., Tomasch, G., Noort, M. van, Rodríguez, J. B., et al., "The Second Flight of the Sunrise Balloon-borne Solar Observatory: Overview of Instrument Updates, the Flight, the Data, and First Results," 2 (2017).

[5] Solanki, S. K., Iniesta, J. C. del T., Woch, J., Gandorfer, A., Hirzberger, J., Alvarez-Herrero, A., Appourchaux, T., Pillet, V. M., Pérez-Grande, I., Kilders, E. S., Schmidt, W., Cama, J. M. G., Michalik, H., Deutsch, W., Fernandez-Rico, G., Grauf, B., Gizon, L., Heerlein, K., Kolleck, M., et al., "The Polarimetric and Helioseismic Imager on Solar Orbiter," A&A **642**, A11 (2020).

[6] Williams, T. L., [The Optical Transfer Function of Imaging Systems, 1st ed.], Routledge, New York (2018).

[7] Boreman, G. D., [Modulation Transfer Function in Optical and Electro-Optical Systems], SPIE, 1000 20th Street, Bellingham, WA 98227-0010 USA (2001).

[8] Huang, K.-Y., Chia, C.-M. and Chang, E., "Optical resolution measurement system for small lens by using slanted-slit method," Optical Measurement Systems for Industrial Inspection VIII **8788**, 705–712, SPIE (2013).
[9] Gonsalves, R. A., "Phase diversity: math, methods and prospects, including sequential diversity imaging," Unconventional Optical Imaging **10677**, 335–345, SPIE (2018).
[10] Tyo, J. S., "Design of Optimal Polarimeters: Maximization of Signal-to-Noise Ratio and Minimization of Systematic Error," Appl. Opt. **41**(4), 619–630 (2002).
[11] Salami, H. and Ross, A. J., "A molecular iodine atlas in ascii format," Journal of Molecular Spectroscopy **233**(1), 157–159 (2005).
[12] Marcy, G. W. and Butler, R. P., "Precision radial velocities with an iodine absorption cell," PASP **104**(674), 270 (1992).
[13] Sanchez, A., Gonzalo, A., Garranzo-García, D., Silva-Lopez, M., Núñez, A., Laguna, H., Cebollero, M., Fernandez-Medina, A. and Alvarez-Herrero, A., "High precision and thermally controlled filter wheel," Proc. SPIE Astronomical Telescopes & Instrumentation, to be published (2022).
[14] Álvarez-Herrero, A., Parejo, P. G. and Silva-López, M., "Fine tuning method for optimization of liquid crystal based polarimeters," Opt. Express, OE **26**(9), 12038–12048 (2018).
[15] del Toro Iniesta, J. C. and Collados, M., "Optimum Modulation and Demodulation Matrices for Solar Polarimetry," Appl. Opt. **39**(10), 1637–1642 (2000).